The ill-defined parameters of the building internal pressure dynamics problem

R.N. Sharma[1]

[1]Department of Mechanical Engineering
The University of Auckland, Auckland 1142, New Zealand

Abstract

A review of literature is carried out on the building internal pressure dynamics problem to show that a wide range for the opening parameters, namely the loss and inertia coefficients, C_L and C_I, are in use. An analysis in the present study shows the fluctuating and peak internal pressure coefficients can vary over the range of these ill-defined parameters by as much as 40%. This is not satisfactory and further studies into these ill-defined parameters of the internal pressure problem are recommended.

Introduction

The safety of a building during the passage of windstorms depends on the characteristics of both internal as well as external pressures, since these can combine to produce extreme loads on elements of the building envelope. Traditionally, building designers and wind engineers focussed largely on the characteristics of building external pressure, hence a large body of literature exists in this area. Internal pressure on the other hand has received relatively less attention even though its importance has continually been highlighted during the aftermath of severe windstorms around the globe [1].

Non-neutral internal pressure in buildings may be induced by the wind through leakage's or permeability of the envelope; through dominant openings; and through the flexibility of the envelope. Of particular interest under windstorm conditions is the generation of internal pressure fluctuations through dominant openings. Such openings may be created by impact of wind-borne debris. Sudden breakage of windows and doors in this manner is not uncommon in severe windstorms. Similarly, intentional opening of doors for escape during windstorms is also common.

There are two issues of concern once a dominant opening has been created. First is the internal pressure overshoot, if any, in the ensuing transient response to a suddenly created opening that presents a sudden change in pressure at the opening. Second is the subsequent response including any resonant response of the building cavity to the turbulent wind via the fluctuations in external pressure at the opening. Both these mechanisms could produce peak internal pressure values that could combine with envelope (e.g. roof) external pressure to generate extreme loading on the envelope. Similarly, the so-called steady-state response, or the subsequent response after the transients if any, have died down, could involve Helmholtz resonance effects, that could produce (a) peak internal pressures that are higher than the peak values for external pressure at the opening; and (b) significant fluctuations in internal pressure thus enhancing fatigue loading on the components of the building.

The characteristics of internal pressure will depend upon the characteristics of the driving external pressure at the opening, as well as the frequency response characteristics of the building cavity determined by the opening area, internal volume, background leakage, secondary openings, partitioning, and the flexibility of the envelope, if any. Since a large body of literature

already exists as far as external pressures are concerned, and that wind loading codes have comprehensive provisions for them, the characteristics of external pressure required for the prediction of internal pressure characteristics are readily available. On the other hand, following a novel treatment of the internal pressure problem by Holmes [2], several researchers [3-10] amongst others, have since greatly increased the understanding of the frequency response characteristics of building cavities and the characteristics of internal pressure induced through dominant openings. Whilst this may be the case, however, even for the apparently simplest case of a rigid, non-porous, single compartment building with a dominant opening, there still remains a number of aspects of the problem that require further investigation.

Firstly, there are a number of variations of the governing equation for internal pressure that are in use at present. Secondly, the coefficients used in the governing equation also vary quite significantly from one study to another. The internal pressure response computed using the governing equations are strongly dependent on these coefficients. Thirdly, a number of different methodologies are in use to predict the RMS response of and gust factors for internal pressure, and not all are in agreement with each other.

It is therefore the purpose of this paper to (a) review the governing equations for internal pressure, for the case of a rigid, non-porous, and single compartment building with a dominant opening, (b) collate data and present discussions on the ill-defined parameters of the flow through dominant openings in buildings, and (d) conduct numerical modelling of internal pressure fluctuations to establish its sensitivity to the ill-defined parameters of the internal pressure problem.

Governing equation for building internal pressure

The four different formulations for the governing equation in use today have been summarised previously by Sharma et al [11]. The problem to be considered is that of a building cavity with a dominant opening, as shown in Figure 1.
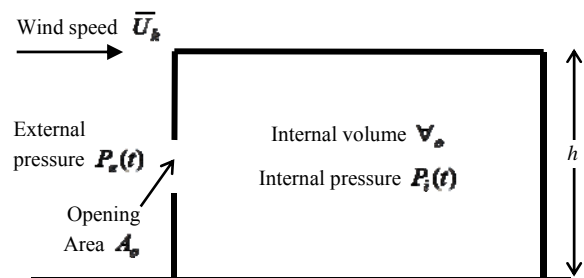
Figure 1. Building with a dominant opening

In the Holmes [2] analogy of the Helmholtz acoustic resonator, the oscillatory airflow through the opening is modelled as an oscillatory air slug of area A_o and length $l_e = \sqrt{\pi A_o/4}$ (i.e. air slug of inertia $= \rho_a A_o l_e$), acting against an air spring consisting of the cavity air. In the Holmes [2] equation,

$$\frac{1}{\omega_{HH}^2}\ddot{C}_{pi} + \frac{1}{C_d^2}\frac{\rho_a \forall_o^2 \bar{q}}{2n^2 A_o^2 P_a^2}\left|\dot{C}_{pi}\right|\dot{C}_{pi} + C_{pi} = C_{pe} \qquad (1)$$

A_o = area of the opening, $\forall_o$ = building cavity volume, C_d = opening discharge coefficient, ρ_a = air density, P_a = ambient pressure, and n = a polytropic exponent. Internal and external pressures are represented by the internal and external pressure coefficients $C_{pi} = C_{pi}(t) = P_i(t)/\bar{q}$ and $C_{pe} = C_{pe}(t) = P_e(t)/\bar{q}$ respectively, where $\bar{q} = \frac{1}{2}\rho_a\bar{U}_h^2$ = reference dynamic pressure, $\bar{U}_h$ = mean ridge-height velocity; and f_{HH} is the Helmholtz resonance frequency of the building cavity given by

$$f_{HH} = \frac{1}{2\pi}\omega_{HH} = \frac{1}{2\pi}\sqrt{\frac{nA_o P_a}{\rho_a l_e \forall_o}} \qquad (2)$$

Using numerical solutions to Equation (1) and parallel experimental testing at model scale, Holmes[2] showed that wind turbulence could excite the building cavity through the opening causing Helmholtz resonance to occur. This manifests as intense oscillations in internal pressure about the Helmholtz resonance frequency, as was evidenced by resonant peaks in internal pressure spectra. Having fixed the effective slug length with $l_e = \sqrt{\pi A_o/4}$, Holmes [2] had to use a polytropic exponent $n = 1.2$ and a discharge coefficient $C_d = 0.15$ in order to match the Helmholtz frequency and the damping (i.e. magnitude of resonant peak) predicted by Equation (1) respectively, to experimental measurements. Equally importantly, Holmes further showed that in order to maintain the correct relative position of the Helmholtz resonance frequency in the wind turbulence spectrum at model-scale, either the model-scale velocity in the wind tunnel needed to match the full-scale velocity, or the model cavity volume needed to be increased (distorted) by a factor equalling the square of the ratio of the full-scale to model-scale velocities.

Liu and Saathoff [3] used the unsteady Bernoulli equation to arrive at an equation very similar to that of Holmes [2], Equation (3),

$$\frac{1}{\omega_{HH}^2}\ddot{C}_{pi} + \frac{1}{C_d^2}\frac{\rho \forall_o^2 \bar{q}}{2\gamma^2 A_o^2 P_a^2}\left|\dot{C}_{pi}\right|\dot{C}_{pi} + C_{pi} = C_{pe} \qquad (3)$$

$$f_{HH} = \frac{1}{2\pi}\omega_{HH} = \frac{1}{2\pi}\sqrt{\frac{\gamma C_c A_o P_a}{\rho_a l_e \forall_o}} \qquad (4)$$

The flow through the opening was assumed to form a vena-contracta, hence their model incorporates a contraction coefficient C_c in the inertia term. This implies that the cross-sectional area of the air slug equals $C_c A_o$ and the inertia of the air jet is then $\rho_a C_c A_o l_e$, with $l_e = \sqrt{\pi A_o/4}$. The contraction coefficient was assumed to be the same as the discharge coefficient, i.e. $C_c = C_d$. Air contractions and expansions in the building cavity were assumed to be fairly rapid and therefore isentropic, hence the specific heat ratio $\gamma = 1.4$ for air was used. Later, Liu and Rhee [4] found from model-scale studies that the contraction or discharge coefficient $C_c = C_d = 0.88$ in order to match the measured Helmholtz frequencies. The damping term was however not examined.

Using the unsteady orifice flow equation with a loss term quantified using an opening loss coefficient C_L being equivalent to $1/C_d^2$, Vickery and Bloxham [6] derived Equation (3),

$$\frac{1}{\omega_{HH}^2}\ddot{C}_{pi} + C_L\frac{\rho \forall_o^2 \bar{q}}{2\gamma^2 A_o^2 P_a^2}\left|\dot{C}_{pi}\right|\dot{C}_{pi} + C_{pi} = C_{pe} \qquad (5)$$

$$f_{HH} = \frac{1}{2\pi}\omega_{HH} = \frac{1}{2\pi}\sqrt{\frac{\gamma A_o P_a}{\rho_a l_e \forall_o}} \qquad (6)$$

which is very similar to Equations (1) and (3). It was argued that since the orifice flow was highly unsteady, it was not likely to form a vena-contracta. The effective length of the air-slug (or air jet) was determined using an inertia coefficient C_I such that $l_e = C_I\sqrt{A_o}$, but using $C_I = \sqrt{\pi/4}$ made $l_e = \sqrt{\pi A_o/4}$ the same as in Holmes [2] and Liu and Saathoff [3]. It was also argued that an orifice loss coefficient $C_L = 2.86$ for steady flow yields acceptable results when the response predicted by Equation (5) were compared with model-scale measurements in the wind tunnel.

Computational fluid dynamics (CFD) modelling technique was applied for the first time by Sharma and Richards [8-9] to study the transient response of building internal pressure, who using parallel model-scale experimental measurements, argued that the governing equation for internal pressure should take the form of Equation (7),

$$\frac{1}{\omega_{HH}^2}\ddot{C}_{pi} + C_L\frac{\rho \forall_o^2 \bar{q}}{2\gamma^2 A_o^2 P_a^2}\left|\dot{C}_{pi}\right|\dot{C}_{pi} + \frac{\mu P L_e \forall_o}{\Delta r\,\gamma A_o^2 P_a}\dot{C}_{pi} + C_{pi} = C_{pe} \quad (7)$$

$$f_{HH} = \frac{1}{2\pi}\omega_{HH} = \frac{1}{2\pi}\sqrt{\frac{\gamma C_c A_o P_a}{\rho_a l_e \forall_o}} \qquad (8)$$

It was shown that flow separation and a contracted region was indeed formed past the opening, confirming the assumptions of Liu and Saathoff [3]. Therefore it was appropriate to include a contraction coefficient C_c in the inertia term, so that the inertia of the air jet was $\rho_a C_c A_o l_e$. Furthermore, measurements and CFD modelling revealed that the losses in the system consisted of an additional linear damping component, which was represented by the $(\mu P l_e \forall_o/\Delta r\gamma A_o^2 P_a)\dot{C}_{pi}$ term (where P = perimeter of the opening) in Equation (7). This was believed to arise from viscous shear stresses around the opening and was shown to be only important at model-scale unless the opening contained a significant neck. In addition, following Stathopoulos and Luchian [5], the effective air jet length l_e was quantified using $l_e = l_o + C_I\sqrt{A_o}$ in which l_o = thickness of the opening. Experimental measurements suggested that C_I ranged between 0.66 and 0.98 depending on the location of the opening [8]. It was also shown that the loss coefficient could range between 1.2 and 2.8, and that the contraction coefficient should be $C_c = 0.6$ for a thin orifice type opening when $l_o/d_o \ll 1$, where $d_o = \sqrt{4A_o/\pi}$ is the effective opening diameter; or $C_c = 1.0$ for a long opening when $l_o/d_o \geq 1$.

Loss and inertia coefficients

Various writers such as Ginger et al [9] and Oh et al [10] have tended to use the Holmes [2] or Vickery and Bloxham [6] formulation for the governing equation, however with the definition for l_e ranging from $l_e = C_I\sqrt{A_o}$ to $l_e = l_o + C_I\sqrt{A_o}$. Others, for example Sharma and co-workers [7-8, 11], have tended to use a combination of the former as described by Equation (7). As such, there is some uncertainty regarding the exact formulation to use for the internal pressure equation, however, as long as the parameters have been defined properly,

the choice of the equation would probably not matter a great deal, say, in the prediction of peak internal pressures.

An even greater uncertainty appears to exist with regards the values for the loss and inertia coefficients to be utilised, as summarised in Table 1. While loss coefficients C_L (some assuming this equals $1/C_d^2$) can range between 2.5 and 45 (up to 18 x the lowest value), the inertia coefficient C_I appears to have much smaller variability, ranging 0.89 to 1.55 (up to 2 x lowest value). To understand the significance of these large variations of the poorly defined parameters, the sensitivity of the standard deviation and peak internal pressure coefficients predicted using the governing equation(s) to these parameters is examined next.

Table 1. Parameters of the internal pressure equation for buildings / building models with a dominant opening, from experimental studies

Reference	Eqn	Opening location	Wall area A_w (m²)	Opening geometry	Opening area A_o (m²)	Contr'n coeff C_c	Discharge coeff C_d	Loss coeff C_L	Poly-tropic exponent	Effective length l_e	Cavity volume V_o (m³)	Thickness l_o	l_e/l_o	Inertia coefficient C_I	f_{HH} meas'd	f_{HH} calc'd	Investigation type
Holmes [2]	(1)	Centre of windward wall	~0.035	Rectangular	1.066x10⁻⁴ 5.386x10⁻⁴ 1.618x10⁻³ 6.473x10⁻³		0.15	44.4 2.78	1.2		0.0025	6mm	0.47 0.21 0.12 0.06	0.89	115 160 235 315		WT Analytic
Liu and Rhee [4]	(3)	Centre of windward wall	0.045	1cm x 1cm 2cm x 2cm 3cm x 3cm 4cm x 4cm	1 x 10⁻⁴ 4 x 10⁻⁴ 9 x 10⁻⁴ 16 x 10⁻⁴	0.88 av (0.75-0.99)			1.4		5.68x10⁻³	6mm	0.60 0.30 0.20 0.15	0.89	68 95 – 103 120 – 127 144	72 102 125 144	WT
Statthopoulos and Luchian [5]	(3)	Centre of windward wall	0.023	Rectangle window	4 x 10⁻⁶ 6 x 10⁻⁶ 10 x 10⁻⁶ 20 x 10⁻⁶	0.6	0.6	2.78	1.4	$L_o + C_I\sqrt{A_o}$	7 x 10⁻⁴	3mm	1.50 1.22 0.95 0.67	0.86 (I) 0.89 (O)			WT
Vickery and Bloxham [6]	(5)	Centre of windward wall	0.027	<20mmφ 25mmφ	<3.14x10⁻⁴ 4.909x10⁻⁴		0.7 0.81-1.04 (in - out)	2.04 1.56 – 0.92	1.4	$C_I\sqrt{A_o}$	0.025	19mm	1.30 1.04	1.05–1.35¹ 1.55¹			WT Analytic
Sharma and Richards [7]	(7)	- Centre of cylinder - Door	0.0177 0.0147	19mmφ 43mmx18mm	2.835x10⁻⁴ 7.74x10⁻⁴	1.0 0.6		1.50 2.80#	1.4	$L_o + C_I\sqrt{A_o}$	3.879x10⁻³ 3.042x10⁻³	60mm 6mm	3.56 0.22	0.93¹ 1.19¹¹	53 139		WT CFD Analytic
Sharma and Richards [8]	(7)	- Centre of cylinder - Door	0.0177 0.0147	25mmφ 43mmx18mm	4.909x10⁻⁴ 7.74x10⁻⁴	1.0 0.6		1.50# 1.20#	1.4	$L_o + C_I\sqrt{A_o}$	3.803x10⁻³ 3.042x10⁻³	19mm 6mm	0.86 0.22	0.95¹¹ 1.24¹¹	97 136		WT CFD Analytic
Ginger et al [9]	(1,5)	- Window - Door	36.3	2‰* 5‰*	0.8 2.0	0.35 0.15		8.2 45	1.4		1175	50mm 100mm	0.06 0.07	0.89	1.58 2.00		Full scale
Oh et al [10]	(5)	- Door & - Window - Window	0.0465	81mmx19mm 14.3mmφ 8.97mmφ	1.553x10⁻³ 1.606x10⁻⁴ 6.319x10⁻⁵	0.63		2.5	1.4	$L_o + C_I\sqrt{A_o}$	0.18	14.7mm	0.37& 1.16 1.85	0.89			WT Analytic

* $100\% \times A_o / A_w$
† Based on Helmholtz frequency measurements where $f_{HH}=\sqrt{\gamma A_o P_a/\rho_a l_e V_o}/2\pi$
†† Based on Helmholtz frequency measurements where $f_{HH}=\sqrt{\gamma A_o P_a/\rho_a l_e V_o}/2\pi$, $l_e'=l_e/C_o=l_o+C_I\sqrt{A_o}$
# Based on damping in transient responses obtained from experimental tests and CFD modelling; refer Equation (7); where linear damping is quantified separately
& This door is not in the vicinity of the floor inside the model due to additional cavity for volume distortion.

Numerical modelling details

The governing equation for internal pressure, Equation (6) without the linear damping term was solved using a 4th order Runge-Kutta scheme for a typical building cavity – opening combination, under strong wind conditions. The required external pressure forcing function was derived using an inverse FFT technique utilising a spectrum for wind turbulence and external pressure admittance function of Sharma and Richards [12].

Building

A typical low rise building having the following characteristics was considered for the numerical analysis:

Building: $\forall_o = 500$m³, Wall height $h = 4$m, Width $w = 9$m
Opening: $A_o = 2$m², $l_o = 0.1$m, $l_e = l_o + C_I\sqrt{A_o}$, $C_c = 0.6$
At wall centre, centred at $x = w/2$, $y = h/2$

Wind characteristics

Air properties: $\rho_a = 1.2$kg/m³, $P_a = 101{,}300$Pa, $\gamma = 1.4$
Wind / terrain: $\bar{U}_h = 25.6$m/s, $\bar{U}_z/U_* = 2.5\ln(z/z_o)$
$U_* = 1.93$m/s, $z_o = 0.02$m
Turbulence: $I_{u,z} = 1/\ln(z/z_o)$
$S_u(f) = 105U_*^2(z/\bar{U}_z)(1 + 33fz/\bar{U}_z)^{-5/3}$

External pressure

Mean: $\bar{C}_{pe} = 0.68$ (mean pressure coefficient)
Spectrum: $S_{Cpe}(f) = (2\bar{C}_{pe}/\bar{U}_h)^2|\chi_{pe}|^2 S_u(f)$
Admittance: $|\chi_{pe}|^2 = (1 + 8(n_1\sqrt{\bar{x}\bar{y}})^2)^{-0.8}(1 + 15n_2^2)^{-0.9}$
$n_1 = f\sqrt{wh}/\bar{U}_h$, $n_2 = f\sqrt{A_o}/\bar{U}_h$
$\bar{x} = x/(w/2)$, $\bar{y} = y/h$

Internal pressure

Internal pressure coefficients were obtained from the equation,

$$\frac{1}{\omega_{HH}^2}\ddot{C}_{pi} + C_L\frac{\rho\forall_o^2\bar{q}}{2\gamma^2 A_o^2 P_a^2}|\dot{C}_{pi}|\dot{C}_{pi} + C_{pi} = C_{pe} \qquad (9)$$

$$f_{HH} = \frac{1}{2\pi}\omega_{HH} = \frac{1}{2\pi}\sqrt{\frac{\gamma C_c A_o P_a}{\rho_a l_e \forall_o}} \qquad (10)$$

for the following ranges of the loss and inertia coefficients:

Loss coefficient: $C_L = 2.5, 5, 10, 20, 45$
Inertia coefficient: $C_I = 0.7, 0.9, 1.0, 1.25, 1.55$

Simulated wind and pressure characteristics

A simulated wind speed, and external and internal pressure coefficient (C_{pe} and C_{pi}) time series are shown in Figures 2 and 3
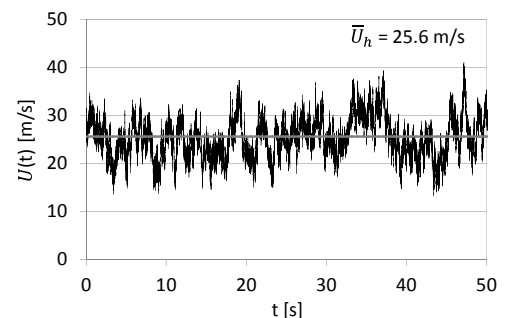
Figure 2. Simulated wind speed time series
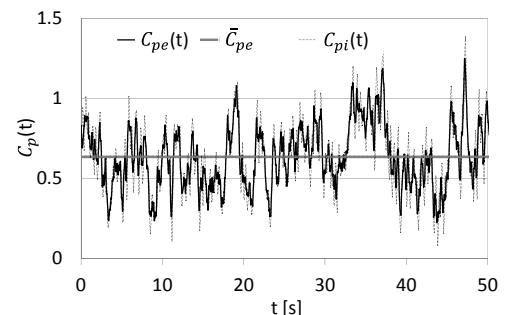
Figure 3. Simulated pressure coefficients, $C_L = 10$, $C_I = 0.7$

respectively. Figure 3, which is for $C_L = 10$ and $C_I = 0.7$ demonstrates the enhancement of fluctuations in internal pressure due to Helmholtz resonance, as the excursions away from the mean level and the peaks in C_{pi} are higher than those in C_{pe}.

Sensitivity of peak and fluctuating internal pressure to loss and inertia coefficients

The sensitivity of internal pressure on the opening loss and inertia coefficients, C_L and C_I, for the building cavity with the fixed opening area, are shown in Figures 4 and 5 below.

Plots of the ratio of the rms internal pressure coefficient to rms external pressure coefficient $\tilde{C}_{pi}/\tilde{C}_{pe}$ in Figure 4 reveal a very strong correlation between internal pressure fluctuations and C_L. The governing equation shows that increasing the loss coefficient C_L increases the damping of the internal pressure system, hence decreases the cavity response, resulting in decreased internal pressure fluctuations. Since internal pressure fluctuations are driven through the opening by the external pressure fluctuations, a decreased response means the ratio $\tilde{C}_{pi}/\tilde{C}_{pe}$ decreases as well. As C_L is increased from 2.5 to 45, the $\tilde{C}_{pi}/\tilde{C}_{pe}$ ratio decreases by between 30-40% depending on the inertia coefficient C_I. Plots of the ratio of the peak internal pressure coefficient to peak external pressure coefficient $\hat{C}_{pi}/\hat{C}_{pe}$ in Figure 5 reveal very similar sensitivity to C_L. As C_L is increased from 2.5 to 45, the peak pressure coefficient ratio $\hat{C}_{pi}/\hat{C}_{pe}$ decreases by approximately 20% except when $C_I = 0.7$, when the decrease is less than 10%.

On the other hand, the sensitivity of internal pressure on the inertia coefficient C_I is not as pronounced. This is due to the independence of the damping term on C_I. The inertia term is however dependent on C_I and it influences the resonance frequency f_{HH}. Over the range of possible values for C_I, the f_{HH} varies between 2.6 to 1.8Hz. As f_{HH} decreases with C_I, the energy available in the onset wind turbulence at the resonance frequency for excitation increases only slightly, hence the increase in $\tilde{C}_{pi}/\tilde{C}_{pe}$ with C_I is not as significant as that observed with the decrease in C_L. Over the C_I range 0.7-1.55, the increase in $\tilde{C}_{pi}/\tilde{C}_{pe}$ is about 10%. Figure 5 shows that the sensitivity of peak internal pressure to C_I is even less significant, except at the lowest values of C_L.
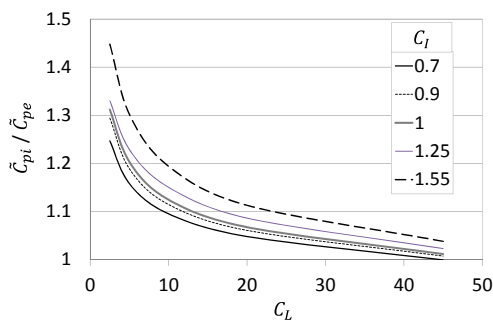
Figure 4. Rms pressure coefficient ratios $\tilde{C}_{pi}/\tilde{C}_{pe}$ versus C_L and C_I
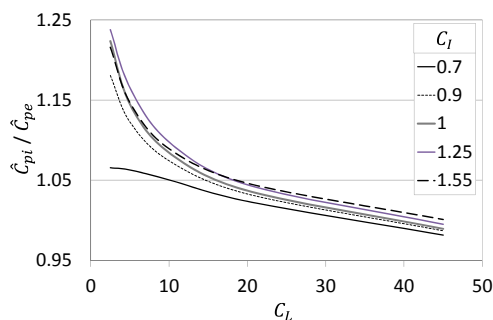
Figure 5. Peak pressure coefficient ratios $\hat{C}_{pi}/\hat{C}_{pe}$ versus C_L and C_I

Conclusions

The wind resistant design of a building relies on our ability to accurately predict the characteristics of internal pressure, especially that which is induced through dominant openings. This ability is limited at the present time largely because of the little attention that internal pressure has received. As a result, the literature shows a wide range for the opening parameters, namely the loss and inertia coefficients, C_L and C_I, in use. The analysis in the present study shows the rms and peak internal pressure coefficients can vary by as much as 40%. Clearly, this is not satisfactory, and further studies into these ill-defined parameters of the internal pressure problem are recommended.

References

[1] Walker, G. R., Report On Cyclone Tracy- Effect On Buildings, Department of Housing and Construction – Australia, 3 Volumes, 1974.

[2] Holmes, J. D., Mean and fluctuating pressures induced by wind, *Proc. of the 5th International Conference on Wind Engineering*, Colorado State University 1979, Peragmon, Oxford, 1980, 435-450.

[3] Liu, H. and Saathoff, P. J., Building internal pressure: sudden change, *Journal of the Engineering Mechanics Division*, 107 (EM2), 1981, 309-321.

[4] Liu, H. and Rhee, K. H., Helmholtz oscillation in building models, *Journal of Wind Engineering & Industrial Aerodynamics*, 95, 1988, 755-779.

[5] Stathopoulos, T. and Luchian, H. D., Transient Wind-Induced Internal Pressures, *Journal of the Engineering Mechanics Division*, ASCE, 115 (EM7), 1989, 1501-1513.

[6] Vickery, B. J. and Bloxham, C., Internal pressure dynamics with a dominant opening, *Journal of Wind Engineering & Industrial Aerodynamics*, 41, 1992, 193-204.

[7] Sharma, R. N. and Richards, P. J., Computational modelling of the transient response of building internal pressure to a sudden opening, *Journal of Wind Engineering and Industrial Aerodynamics*, 72, 1997, 149-161.

[8] Sharma, R. N. and Richards, P. J., Computational modelling in the prediction of building internal pressure gain functions, *Journal of Wind Engineering and Industrial Aerodynamics*, 67-68, 1997, 815-825.

[9] Ginger, J. D., Mehta, K. C., Yeatts, B. B., Internal pressures in a low-rise full-scale building, *Journal of Wind Engineering & Industrial Aerodynamics*, 72, 1997, 163 174.

[10] Oh, J. H., Kopp, G. A. and Inculet, D. R., The UWO contribution to the NIST aerodynamic database for wind loads on low buildings: Part 3. Internal pressures, *Journal of Wind Engineering & Industrial Aerodynamics*, 29, 2007, 293-302.

[11] Sharma, R. N., Mason, S., and Driver, P., Scaling methods for wind tunnel modelling of building internal pressures induced through openings", *Wind and Structures*. 13(4), 2010, 363-374

[12] Sharma, R. N. and Richards, P. J., The multi-stage process of windward wall pressure admittance, *Journal of Wind Engineering and Industrial Aerodynamics*, 92, 2004, 1191-1218..